URSI GASS 2020, Rome, Italy, 29 August - 5 September 2020

Rotational Artefact Removal for Radar-based Breast Imaging: Effects on Image Quality

Declan O'Loughlin*(1)(2), Hamza Benchakroun(2) and Aoife Lowery(1)
(1) School of Medicine, National University of Ireland Galway, Ireland.
(2) Electrical and Electronic Engineering, National University of Ireland Galway, Ireland.

Abstract

Radar-based breast imaging has shown promise as an imaging modality for early-stage cancer detection, and clinical investigations of two commercial imaging systems are on-going. Many imaging algorithms have been proposed, which seek to improve the quality of the reconstructed microwave image to enhance the potential clinical decision. However, a large artefact caused by the interface between the skin and breast interior can obscure reflections from the breast interior and, hence, tumour detection. Rotational subtraction is commonly employed to remove this artefact, however, limited work has examined the optimal parameters for rotational subtraction. In this work, the theoretical basis for rotational subtraction is examined, and the potential negative effects on image quality identified. Overall, this work suggests that it is important that the parameters of rotational artefact removal be optimised to improve radar-based breast image quality.

1 Introduction

In recent years, microwave breast imaging has seen increasing use in early-stage clinical trials [1]–[4], including commercial systems developed by two competing companies [2], [5], [6]. While the indications from these preliminary studies are promising, a number of technical and clinical questions remain which may hinder the clinical adoption of the technology.

Due to the dielectric properties of skin and the adipose layer immediately underneath, a large reflection is caused at the skin interface which may be orders of magnitude greater than any tumour reflections [7]. Although many algorithms exist for image reconstruction [8], many exploit the similarity of the skin response at neighbouring antenna locations to remove the skin reflection artefact [9].

Rotational subtraction has been used in the largest clinical trial to date and many experimental systems [2], [6], [10]. The key assumption of rotational subtraction is that the tumour is not on the axis of rotation, and the tumour response will be preserved after subtraction of the rotated signals. However, few analytical, numerical, experimental or patient studies have examined the impact rotational subtraction may have on the image. Similarly, the optimal angle of rotation has not been studied.

In this work, an analytical model is used to estimate the impact that rotational subtraction may have on the image. The potential impact on image amplitude and localisation are examined, and this analysis identifies future work which could better inform system design. The rest of this paper is structured as follows: the analytical model is presented in Section 2; the results are shown in Section 3 and Section 4 concludes the paper.

2 Methods

In general, the electromagnetic scattering can be calculated from the scattering equation [11] which can be written as:

$$\mathbf{E}(\mathbf{r}') = \mathbf{E}^i(\mathbf{r}') + k^2 \iiint_{\mathscr{D}} \chi(\mathbf{r}') G_b(\mathbf{r}', \mathbf{r}) \cdot \mathbf{E}(\mathbf{r}) \, \mathrm{d}\mathbf{r} \quad (1)$$

where the total field, $\mathbf{E}(\mathbf{r})$, is the superposition of the incident field, $\mathbf{E}(\mathbf{r})$ and the volume integral of the total field times the Green's function of the medium, $G_b(\mathbf{r}', \mathbf{r})$, and the contrast function, $\chi(\mathbf{r})$, over the imaging domain, $\mathscr{D}$, with background wavenumber, k. As the scattering equation is non-linear, the Born approximation is often used, where the total field is approximated by the incident field for the purposes of evaluating the scattered field [12].

In this work, a homogeneous background medium with N antennas located at $\mathbf{a}_n$ spaced evenly around a ring of radius R is considered. No skin is included in the model as it is assumed that the skin is removed completely by the artefact removal. The tumour is represented by a point scatterer at $\mathbf{r}_T$ within the ring of antennas of contract χ_T. Given the homogeneous background, the incident field at $\mathbf{r}$ in the domain can be evaluated as the solution to the wave equation for a point source at $\mathbf{a}$ or:

$$\mathbf{E}^i_{\mathbf{a}}(\mathbf{r}, \omega) = \frac{P(\omega)}{\|\mathbf{r} - \mathbf{a}\|} \exp\left[-ik \|\mathbf{r} - \mathbf{a}\|\right] \quad (2)$$

where ω is the angular frequency of the incident wave, $P(\omega)$ is the amplitude at that frequency and k is the wavenumber of the background medium.

Substituting Equation (2) into Equation (1) and assuming that $\chi(\mathbf{r}) = \delta(\mathbf{r} - \mathbf{r}_T)$, the scattered field received at antenna $\mathbf{a}$ for incident field transmitted from the same antenna can

be approximated as:

$$\mathbf{E_a}(\mathbf{a},\omega) = \frac{\chi f \sqrt{\varepsilon_r} P(\omega)}{4c_0 \|\mathbf{a}-\mathbf{r}_T\|^2} \exp\left[-2ik\|\mathbf{a}-\mathbf{r}_T\|\right] \quad (3)$$

for medium with relative permittivity ε_r, speed of light c_0, wavenumber k and incident field frequency of f.

The scattered signals are processed by the Delay-and-Sum (DAS) algorithm, which can be written as:

$$I(\mathbf{r}) = \sum_{\Omega}\sum_{A}\sum_{A} \mathbf{E}'_{\mathbf{a}}(\mathbf{a},\omega) \exp\left[\frac{2i\omega}{c_0}\sqrt{\varepsilon'_r}\|\mathbf{a}-\mathbf{r}\|\right] \quad (4)$$

where the image amplitude $I(\mathbf{r})$ at the point $\mathbf{r}$ is calculated from the artefact removed signals, $\mathbf{E}'_{\mathbf{a},\mathbf{a}}(\mathbf{r})$, collected at antenna locations $\mathbf{a} \in A$ at frequencies $\omega \in \Omega$ and an assumed relative permittivity of the background medium ε_r.

The artefact removed signals are calculated using rotational artefact removal, that is, the artefact removed signal for antenna location $\mathbf{a}$ is the scattered field recorded at $\mathbf{a}$ ($\mathbf{E_a}(\mathbf{a},\omega)$) minus the scattered field recorded at $\mathbf{a}'$ ($\mathbf{E_{a'}}(\mathbf{a}',\omega)$), where the rotated location $\mathbf{a}'$ is rotated an angle of θ about the centre of the imaging domain from the original location $\mathbf{a}$.

3 Results

The results for the simplified model presented in the previous section are divided into a number of parts:

1. firstly, the image amplitude as a function of rotation and tumour location is examined in Section 3.1;
2. secondly, the images are qualitatively compared in Section 3.2.

For the following results, the imaging domain has a radius of 8 cm with 41 antennas evenly spaced around the ring. The image is formed with 21 frequency points linearly spaced between 2 GHz and 4 GHz. The relative permittivity of the lossless medium is $\varepsilon_r = 9$. All images were created using the MERIT toolbox in the frequency domain [13].

3.1 Image Amplitude

In this section, the relative amplitudes of the images formed with rotational subtraction at different angles and the ideal image is shown in Figure 1.

As can be seen in Figure 1, the relative amplitudes of the images can change considerably over the range of rotation angles. As is expected, for point scatterers close to the centre (such as 1 cm from the centre), the amplitude of the image is lower than the corresponding ideal image until almost 30°. However, as the point scatterer moves further away from the centre of the imaging domain, the amplitude of the image approaches that of the ideal image much sooner. For example, for a point scatterer 3 cm from the centre, the image reconstructed using rotational subtraction has the same amplitude as the ideal image at 10° of rotation.

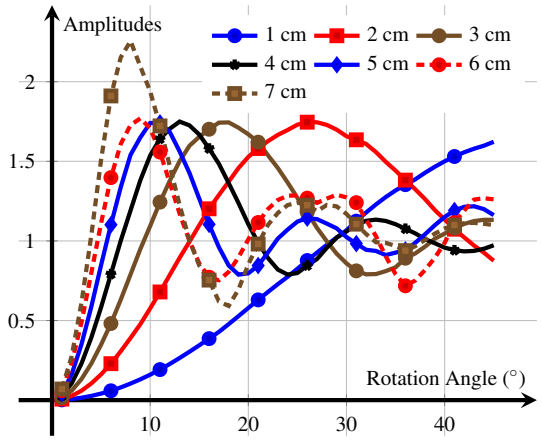

Figure 1. The relative amplitudes of the image formed with rotational subtraction using a given rotation angle for tumours between 1 cm and 7 cm from the centre of the imaging domain. For each tumour location, the relative amplitude of the image formed with rotational subtraction compared to the ideal image for that location is shown.

As the rotation angle increases, the artefact removed image increases in amplitude when compared with the ideal image. This effect is related to the coherent addition that is the fundamental basis of DAS. Depending on the wavelengths used, and the distances between the original and rotated antenna positions to the tumour, different peaks of the tumour responses can overlap creating additional phantom energy at the tumour location.

3.2 Qualitative comparison

In this section, the images formed as the rotation angle changes are compared qualitatively. Four images are shown in Figure 2: the ideal image, and the image with rotational subtraction at three different angles. The three angles are chosen from Figure 1 as the image where the amplitude is equal to the ideal, the image of maximum amplitude and the next local minimum, 9°, 18° and 33° respectively.

Firstly, comparing the localisation of the point scatterer as the rotation angle increase, it can be seen that multiple responses are visible at higher angles of rotation. At lower angles of rotation, the additional response is close to the actual location, but can distort slightly the shape of the point scatterer response. As the angle increases, the additional "echo" grows more distinct from the actual response and could appear as a different object.

Secondly, considering the clutter in the images, more energy can be seen outside of the point scatterer location as

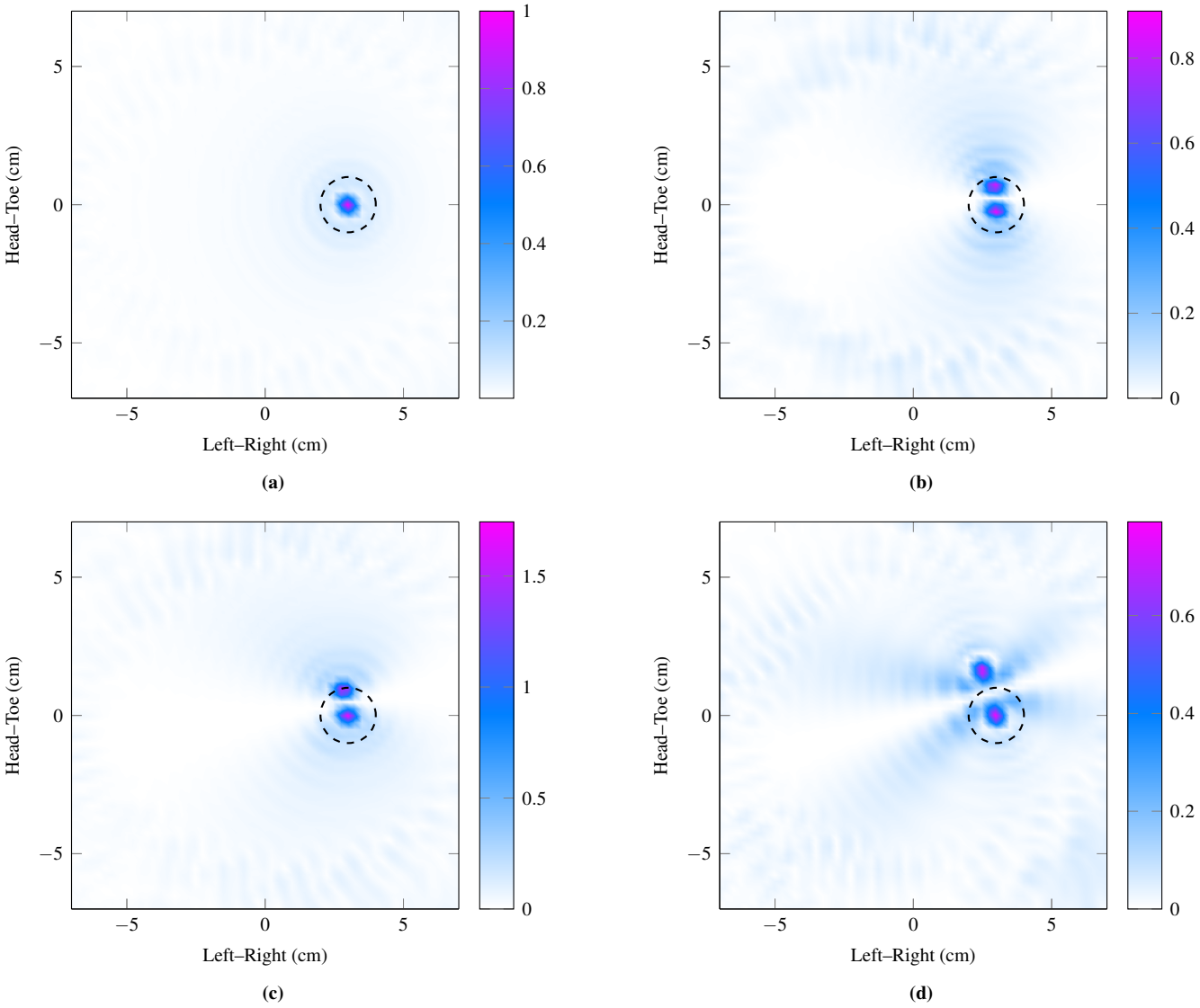

Figure 2. In this figure, the ideal image is shown in (a) and the images formed by rotational subtraction by 9°, 18° and 33° are shown in (b), (c) and (d) respectively. As can be seen, rotational subtraction can create an "echo" due to the differences in distances between the original and rotated antenna locations and the point scatterer. For smaller angles of rotation, this echo is very close to the actual location. The location of the point scatterer is indicated by the dashed circle.

the angle of rotation increases. This is due to additional energy in the signals used for addition caused by differences in distances between the original and rotated antenna positions and the point scatterer location.

4 Conclusions

In this work, a simplified model is used to examine the potential impact of rotational artefact removal on microwave breast images. Even in these simplified scenarios, rotational artefact removal can induce additional artefacts and echos in the images. These results suggest that the optimal angle of rotation should be examined further. Depending on the tumour location and the angle of rotation, the image may be substantially altered in both amplitude and shape by rotational artefact removal even in simplified scenarios.

However, a number of additional complexities exist in patient imaging which may mitigate these results. Firstly, the skin response will not be completely removed by rotation, and the additional energy from this response may obscure any additional clutter caused by the rotation of the tumour response. Secondly, the tumour itself may not be well modelled by a point scatterer, both in terms of physical extent and angular isotropy. Future work should include numerical, experimental and clinical examination of this imaging parameter to determine if this theoretical problem can negatively impact microwave breast imaging quality.

5 Acknowledgements

This work was supported by the Irish Research Council (EPSPD/2019/200; EPSPD/2019/419 and New Foundations).

References

[1] E. C. Fear, J. Bourqui, C. F. Curtis, *et al.*, "Microwave Breast Imaging With a Monostatic Radar-Based System: A Study of Application to Patients," *IEEE Transactions on Microwave Theory and Techniques*, vol. 61, no. 5, pp. 2119–2128, May 2013.

[2] H. Song, S. Sasada, T. Kadoya, *et al.*, "Detectability of Breast Tumor by a Hand-held Impulse-Radar Detector: Performance Evaluation and Pilot Clinical Study," en, *Scientific Reports*, vol. 7, no. 1, Dec. 2017, Art. 16353.

[3] D. O'Loughlin, M. O'Halloran, B. M. Moloney, *et al.*, "Microwave Breast Imaging: Clinical Advances and Remaining Challenges," *Transactions on Biomedical Engineering*, vol. 65, no. 11, pp. 2580–2590, Nov. 2018.

[4] J.-C. Bolomey, "Crossed Viewpoints on Microwave-Based Imaging for Medical Diagnosis: From Genesis to Earliest Clinical Outcomes," en, in *The World of Applied Electromagnetics*, A. Lakhtakia and C. M. Furse, Eds., Cham, Switzerland: Springer International Publishing, 2018, pp. 369–414.

[5] A. Fasoula, L. Duchesne, J. Gil Cano, *et al.*, "On-Site Validation of a Microwave Breast Imaging System, before First Patient Study," en, *Diagnostics*, vol. 8, no. 3, p. 53, Aug. 2018.

[6] A. W. Preece, I. J. Craddock, M. Shere, *et al.*, "MARIA M4: Clinical evaluation of a prototype ultrawideband radar scanner for breast cancer detection," *Journal of Medical Imaging*, vol. 3, no. 3, p. 033 502, Jul. 2016.

[7] R. C. Conceição, J. J. Mohr, and M. O'Halloran, Eds., *An Introduction to Microwave Imaging for Breast Cancer Detection*, 1st ed., ser. Biological and Medical Physics, Biomedical Engineering. Switzerland: Springer International Publishing, 2016.

[8] D. O'Loughlin, B. L. Oliveira, M. A. Elahi, *et al.*, "Parameter Search Algorithms for Microwave Radar-Based Breast Imaging: Focal Quality Metrics as Fitness Functions," *Sensors*, vol. 17, no. 12, Dec. 2017, Art. 2823.

[9] M. A. Elahi, D. O'Loughlin, B. R. Lavoie, *et al.*, "Evaluation of Image reconstruction algorithms for confocal microwave imaging: Application to patient data," *Sensors*, vol. 18, no. 6, May 2018, Art. 1678.

[10] D. O'Loughlin, B. L. Oliveira, A. Santorelli, *et al.*, "Sensitivity and specificity estimation using patient-specific microwave imaging in diverse experimental breast phantoms," *IEEE Transactions on Medical Imaging*, vol. 38, no. 1, pp. 303–311, Jan. 2019.

[11] N. K. Nikolova, "Microwave Biomedical Imaging," *Wiley Encyclopedia of Electric and Electronics Engineering*, pp. 1–22, Apr. 2014.

[12] R. Solimene, A. Cuccaro, G. Ruvio, *et al.*, "Beamforming and holography image formation methods: An analytic study," en, *Optics Express*, vol. 24, no. 8, p. 9077, Apr. 2016.

[13] D. O'Loughlin, M. A. Elahi, E. Porter, *et al.*, "Open-source software for microwave radar-based image reconstruction," in *Proceedings of the 12th European Conference on Antennas and Propagation (EuCAP)*, London, the UK: IEEE, Apr. 2018.